Sn-9Zn-*x*Ag 无铅钎料润湿性能及焊点力学性能

陈文学， 薛松柏， 王 慧， 王俭辛
（南京航空航天大学 材料科学与技术学院，南京 210016）

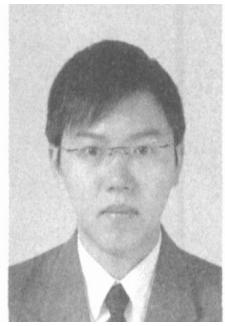

陈文学

摘 要：研究了合金元素 Ag 的添加量对 Sn-9Zn 无铅钎料润湿性能及其焊点力学性能的影响. 结果表明，当 Ag 元素的添加量（质量分数）为 0.3%时，钎料具有最好的润湿性能，焊点的力学性能最佳，焊接接头的断口形貌显示钎料与铜基板接头断口处有明显的韧窝，是典型的韧性断裂；当 Ag 元素的添加量（质量分数）为 0.5%～1.0%时，钎料的润湿性能下降，当 Ag 元素的添加量（质量分数）增加到 1.0%时，焊点的力学性能有所下降，在断口的韧窝底部有大颗的 Cu-Zn，Ag-Zn 金属间化合物. 因此，Sn-9Zn 无铅钎料中合金元素 Ag 的最佳添加量（质量分数）为 0.3%.

关键词：Ag 元素；无铅钎料；润湿性能；力学性能
中图分类号：TG425 文献标识码：A 文章编号：0253－360X(2009)06－0075－04

0 序 言

铅对人体的危害已受到世界各国的重视，随着欧盟、美、日等国限制生产和进口含铅电子产品的相关法规的陆续实施，有关研发、应用无铅钎料的研究工作越来越受到人们的重视[1].

目前研究的无铅钎料主要有 Sn-Ag，Sn-Cu，Sn-Bi，Sn-Zn 等二元系合金，Sn-Ag-Cu，Sn-Ag-Bi，Sn-Zn-Bi，Sn-Zn-Ag 等三元系合金[2]. 其中 Sn-Zn 系无铅钎料由于原材料来源广泛、价格成本低、共晶熔点（198 ℃）与 Sn-37Pb 的熔点（183 ℃）相近而受到广泛关注，而且共晶 Sn-Zn 无铅钎料具有比 Sn-Pb 钎料更高的焊点抗剪强度，电迁移效应也优于 Sn-Pb，室温下具有比 Sn-Pb 更好的抗疲劳性能[3]. 但是合金中的 Zn 是一种极易被氧化和腐蚀的元素[4]，其离子化倾向相当大，抗氧化能力差，易形成稳定的氧化物，对钎料的润湿性产生很大的影响，同时 Sn-Zn 抗腐蚀性较差. 改善 Sn-Zn 钎料润湿性能的方法通常有两种[5]：一种是开发合适的助焊剂，另一种是在钎料中添加合金元素. 文中设计的合金是以 Sn-9Zn 系为基材，添加合金元素 Ag，对合金的润湿性能及焊点力学性能进行研究，旨在找出合金元素 Ag 在 Sn-9Zn 合金中的适宜添加量.

收稿日期：2009－01－21
基金项目：2006 年江苏省“六大人才高峰”资助项目(06-E-20)

1 试验方法

试验采用 Sn-9Zn 无铅钎料为母合金，添加的 Ag 元素含量见表 1. 采用规格为 30 mm× 5 mm×0.3 mm 的无氧铜片，免清洗助焊剂，日本 Rhesca 公司生产的 SAT-5100 型可焊性测试仪和日本 Rhesca 公司的 STR-1000 微焊点强度测试仪.

表 1 Sn-9Zn 试验钎料中 Ag 元素的添加量（质量分数，%）
Table 1 Ag addition to Sn-9Zn solder alloys

合金序号	Ag 元素的添加量
1	0.0
2	0.1
3	0.3
4	0.5
5	1.0

试验参照日本工业标准 JIS Z 3198《无铅钎料试验方法——第 4 部分：基于润湿平衡及接触角法的润湿性试验方法》(2003)[6] 进行. 将钎料放入 SAT-5100 型可焊性测试仪中，加热使之熔化，呈熔融状态，保持温度为 245 ℃. 然后将处理好的试验铜片浸入免清洗助焊剂中 5 s 后，立刻固定于测试仪的夹具上. 用刮刀除去钎料表面的氧化膜，将铜片以 4 mm/s 的速度垂直浸入钎料中，浸入深度为 2 mm，保持 10 s 后将铜片移出钎料. 从铜片进入钎料的瞬间开始到试件与钎料的脱离，测定了试件所受作用力

随时间的变化曲线.

试验测试了在 245 ℃下,使用免清洗助焊剂,钎料在铜基板上的润湿时间以及润湿力,通过这两个参数来评价钎料的润湿性能.

试验参照日本工业标准 JIS Z 3198《无铅钎料试验方法——第 6 部分:QFP 引线焊点的 45 度角拉脱试验方法》(2003)[6] 进行. 试验时,使用表 1 中的 5 种不同成分的无铅钎料配合适量的钎剂,将 QFP100(扁平封装器件,引脚 100)再流焊接到 FR-4 基板上,然后采用 STR-1000 微焊点强度测试仪来测试不同成分的钎料在相同的焊接条件下焊点的拉伸力.

2 结果和分析

2.1 Ag 对 Sn-9Zn-xAg 系钎料润湿性能的影响

依照 1.2 章节所示的试验标准,在 245 ℃下分别测试了 5 种不同 Ag 元素含量的钎料合金的润湿时间和润湿力,测定结果如图 1 所示.

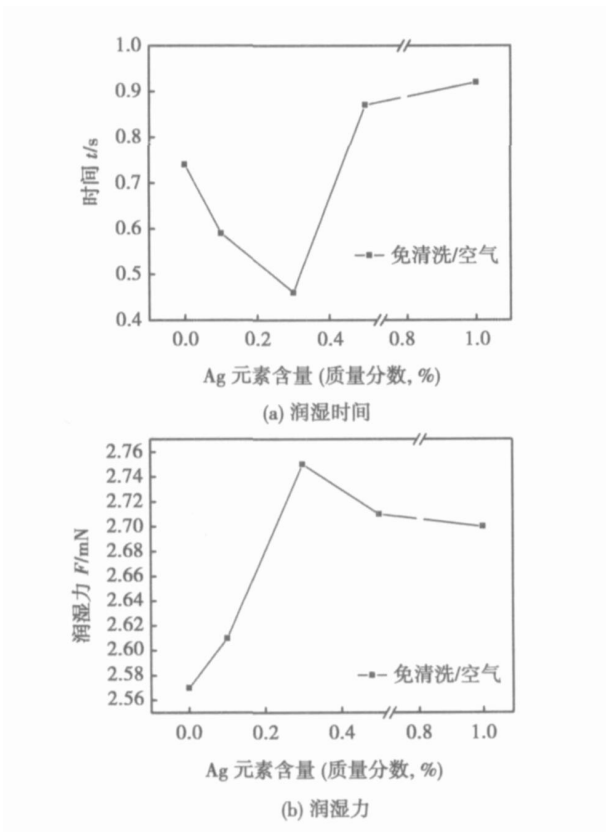

图 1 Ag 元素含量对 Sn-9Zn 无铅钎料润湿性能的影响

Fig. 1 Effects of Ag addition on wettability of Sn-9Zn lead-free solders

由图 1 可以看出,Ag 元素含量在 0.3(质量分数,%)以下时,钎料在铜基板表面润湿时间随着 Ag 含量的增加而减小,润湿力随着 Ag 元素含量的增加而增加. 当 Ag 元素含量为 0.3(质量分数,%)时,润湿时间最短,润湿力最大,钎料的润湿性能达到最佳. Ag 元素的含量继续增加时,润湿时间不断增加,润湿力逐渐减小,钎料的润湿性能下降.

图 2 所示为 Sn-9Zn 和 Sn-9Zn-0.3Ag 两种钎料的热重分析(TGA)曲线在 245 ℃时,加入合金元素 Ag 以后,钎料的抗氧化性能明显增强,从而钎料的润湿性能得到改善.

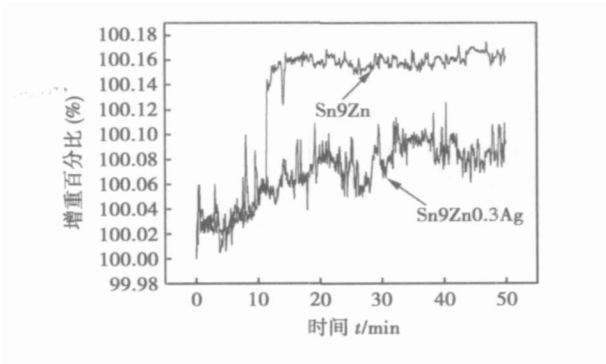

图 2 Sn-9Zn-0.3Ag 钎料和 Sn-9Zn 钎料的热重分析

Fig. 2 TGA results of Sn-9Zn-0.3Ag solder compared to Sn-9Zn solder

当 Ag 元素的添加量在 0.5(质量分数,%)以上时,随着 Ag 元素含量升高,钎料的熔点随之增高[7],钎料熔体的粘滞性增加[8],钎料的流动性降低,钎料的润湿性能恶化.

2.2 Ag 对 Sn-9Zn-xAg 钎料焊点力学性能的影响

依照 1.3 章节的试验方法,得到 QFP 引线焊点的拉伸力,结果如图 3 所示.

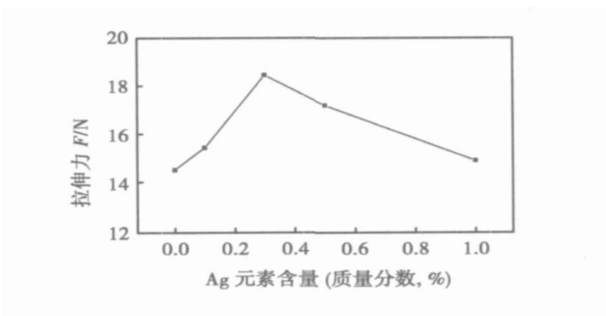

图 3 Ag 元素含量对 Sn-9Zn 无铅钎料焊点力学性能的影响

Fig. 3 Effect of Ag addition on mechanical properties of Sn-9Zn lead-free soldered joints

由图 3 可以看出,Ag 元素含量在 0.3(质量分数,%)以下时,QFP 引线焊点的拉伸力随着 Ag 元素含量的增加而增大. 当 Sn-9Zn 钎料中 Ag 元素含量

增加到0.3(质量分数，%)时，QFP 引线焊点的拉伸力达到最大，随着 Ag 元素含量的继续增加，拉伸力逐渐减小.

图4 所示为不同 Ag 元素含量的 Sn-9Zn 钎料与铜基板间焊接接头的断口形貌.

由图4a，b，c 可知 Sn-9Zn，Sn-9Zn-0.1Ag，Sn-9Zn-0.3Ag 钎料与铜基板接头断口处均有明显的韧窝，是典型的韧性断裂. 相应的 EDS 分析结果表明韧窝处成分主要是 Sn 和少量的 Zn，没有检测到 Cu 和 Ag，说明断裂发生在钎料内部，而且Sn-9Zn-0.3Ag

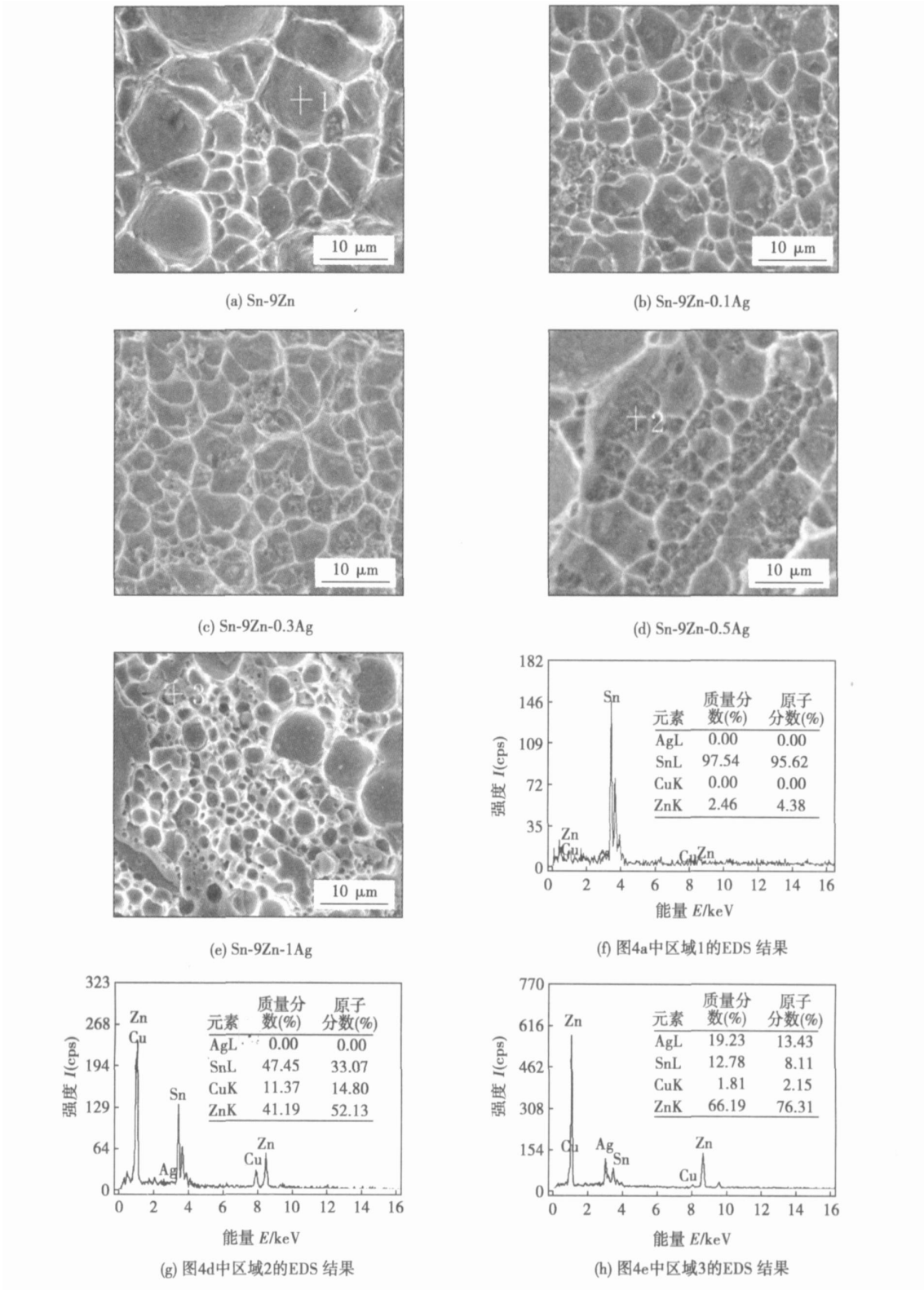

图 4　不同 Ag 元素含量的 Sn-9Zn 钎料与铜基板间焊接接头断口形貌

Fig. 4　Fracture micrographs of joints soldered by Sn-9Zn solders with different amount of Ag addition

钎料内部的韧窝较 Sn-9Zn 钎料更为细小均匀，因而具有更好的力学性能.

图 4d 所示为 Sn-9Zn-0.5Ag 钎料与铜基板焊接接头断口形貌，从图中可以看出在断口处除有韧窝外还有一些区域. 结合能谱分析可知，该区域 Zn 和 Cu 含量较高，按其原子比例推断为界面处形成的 Cu-Zn 金属间化合物. 图 4e 所示为 Sn-9Zn-1Ag 钎料与铜基板焊接接头断口形貌，在钎料处的韧窝底部有大颗的化合物，能谱分析显示其中含有较多的 Ag 元素，说明除含有 Cu-Zn 金属间化合物外，还含有 Ag-Zn 化合物. 金属间化合物本身是较硬而脆的相，在焊接接头受应力作用时易成为应力集中区，因而易成为裂纹萌生和扩展的源头；另外，金属间化合物的晶格与钎料基体晶格很难匹配，在界面处存在缺陷的薄弱区域容易断裂，与此对应，QFP 引线焊点的力学性能有所下降.

3 结 论

(1) Ag 元素的加入可以改善 Sn-9Zn 无铅钎料的润湿性能. 当 Ag 元素的添加量在 0～0.3(质量分数，%)时，钎料的润湿性能改善幅度较大，当 Ag 元素的添加量大于 0.5(质量分数，%)时，钎料的流动性下降，钎料的润湿性能下降.

(2) 当 Ag 元素的添加量达到 0.3(质量分数，%)时，QFP 引线焊点的力学性能达到最佳，断口处有明显的韧窝，是典型的韧性断裂；当 Ag 元素的含量进一步增加时，在钎料处的韧窝底部有大颗 Cu-Zn，Ag-Zn 金属间化合物，QFP 焊点的力学性能有所下降.

参考文献：

[1] 王旭艳，薛松柏，禹胜林，等. 温度与镀层对 Sn-Ag-Cu 无铅钎料润湿性的影响[J]. 焊接学报，2005，26(10)：93－96.
Wang Xuyan，Xue Songbai，Yu Shenglin，*et al*. Effects of temperature and coatings on wettability of Sn-Ag-Cu lead-free solder[J]. Transactions of the China Welding Institution，2005，26(10)：93－96.

[2] Abtewa M，Selvaduray G. Lead-free solders in microelectronics[J]. Materials Science and Engineering R，2000，27(5－6)：95－141.

[3] Chen C M，Huang Y M，Lin C P，*et al*. Effect of temperature on microstructural changes of the Sn-9 wt.% Zn lead-free solder strip under current stressing[J]. Marterials Chemistry and Physics，2009，115(1)：367－370.

[4] 黎小燕，陈国海，马莒生. Sn-Zn 无铅焊料的研究与发展[J]. 电子工业技术，2004，25(4)：150－153.
Li Xiaoyan，Chen Guohai，Ma Jusheng. Research and development of Sn-Zn lead-free solder[J]. Electronics Process Technology，2004，25(4)：150－153.

[5] Chen X，Hu A M，Li M，*et al*. Study on the properties of Sn-9Zn-*x*Cr lead-free solder[J]. Journal of Alloys and Compounds，2008，460(1－2)：478－484.

[6] 王春青，李明雨，田艳红，等. JIS Z 3198 无铅钎料试验方法简介与评述[J]. 电子工艺技术，2004，25(3)：50－54.
Wang Chunqing，Li Mingyu，Tian Yanhong，*et al*. Review of JIS Z3198：Test method for lead-free solders[J]. Electronics Process Technology，2004，25(3)：50－54.

[7] 王 慧，薛松柏，陈文学，等. Ag，Al，Ga 对 Sn-9Zn 无铅钎料润湿性能的影响[J]. 焊接学报，2007，28(8)：33－36.
Wang Hui，Xue Songbai，Chen Wenxue，*et al*. Effect of Ag，Al，Ga addition on wettability of Sn-9Zn lead-free solder[J]. Transactions of the China Welding Institution，2007，28(8)：33－36.

[8] 黄惠珍，黄起森，彭 曙，等. 添加 Ag 对 Sn-9Zn 无铅钎料合金性能的影响[J]. 特种铸造及有色合金，2006，26(3)：179－181.
Huang Huizhen，Huang Qisen，Peng Shu，*et al*. Effects of Ag addition on properties of Sn-9Zn lead-free solder alloys[J]. Special Casting and Nonferrous Alloys，2006，26(3)：179－181.

作者简介：陈文学，男，1985 年出生，硕士研究生. 主要从事微电子焊接技术及无铅钎料研究工作. 发表论文 3 篇.

Email：wenxuechen@nuaa.edu.cn

welding. The distortion of the stiffened plate for the successive welding will occur, but the simultaneous welding won't do. The deflection distortion of welded structure relates to the neutral axis of its structure.

Key words: numerical simulation; welding deformation; welding sequence; neutral axis

Special-purpose welding robot for intersection welding seam

REN Fushen[1,2], CHEN Shujun[1], GUAN Xinyong[1], YIN Shuyan[1] (1. School of Mechanical Engineering and Applied Electronics Technology, Beijing University of Technology, Beijing 100022, China; 2. School of Mechanical Science and Engineering, Daqing Petroleum Institute, Daqing 163318, China). p 59—62

Abstract: The welding seam of intersecting pipes is typical and complicated space welding seam. A new welding robot with 5-degree of freedoms robot is designed with the mixed method of series and parallel for special welding technological requirements of welding seam of intersecting pipes, which realized the one integrated design of organization for robot anchor, motion mechanism, welding gun adjusting mechanism and wire feeder. An automatic centering robot trick with 2-degree of freedom is designed, which realized control to gun position and pose separately. The kinematics model of the welding robot is build, and the real-time control mathematical model of welding gun position, welding gun pose and welding speed is build too for the general welding seam of intersection. The welding result indicates that the anchor is secure and accurate, the controllability during the welding is good, and the control method can satisfy the technological requirement of welding seam of intersection.

Key words: arc welding robot; intersection welding seam; anchor; automatic centering trick

All-fiber optic integration type of weld seam image sensing system

HUANG Minshuang, HUANG Junfen, TANG Jian, JIANG Lipei (Opto-Mechatronic Equipment Technology Beijing Area Major Laboratory, Beijing Institute of Petrochemical Technology, Beijing 102617, China). p 63—66

Abstract: A novel all-fiber optic integration type of weld seam image sensing system with line-structure light projection is put forward, which the optical projection field of line-structure light is produced by integration of an optic transmission fiber and a minitype cylinder lens, and the laser image of weld seam is received with an image transmission fiber bundle. The near-field intensity distribution of the large core quartz fiber-optic transmission surface and the characteristic of the fiber bundle transmitting the laser image of welding seam are analyzed with the ray theory. The theory analysis indicates that the laser transmitted through the large core fiber optic helps to improve the quality of the projection stripe; the great mass of image noise can be filtered after the laser image of weld seam is transmitted by the image transmission fiber optic due to the spatial filtering effect. The experiment results are accordance with the theory analysis in the main.

Key words: optical intensity distribution; spatial filtering; weld seam image; fiber-optic sensor

Development of precise inverter reflow-soldering power supply with waveform control

CAO Biao, FAN Fengxin, ZENG Min, SHAO Lanjuan (Department of Mechanical and Automotive Engineering, South China University of Technology, Guangzhou 510640, China). p 67—70

Abstract: Reflow-soldering is a sophisticated welding method on the electronic components. For precisely controlling the reflow-soldering, the control system adopts PIC18F6585 as the control core and the closed-loop feedback through thermocouple as to control the welding temperature. The language of the control system is written with C language and assembly language. Through the waveform control of different stage and the digital PI algorithm regulation, the power supply achieves precise control of the welding process. Experimental results validate that the control system of the power supply can accurately control the welding pressure, time and temperature, and has obvious advantages in the surface mount technology field.

Key words: reflow soldering; inverter power supply; thermocouple; waveform control

Microstructure and mechanical properties of austenite stainless steel wire joints welded by laser

LI Hongmei, SUN Daqian, WANG Wenquan, XUAN Zhaozhi, REN Zhenan (College of Materials Science and Engineering, Jilin University, Changchun 130025, China). p 71—74

Abstract: Austenite stainless steel thin wires were joined by using pulsed YAG laser welding. The microstructural characteristics and influences of laser welding parameters on microstructures and mechanical properties of joints were investigated by means of optical microscopy and scanning electronic microscopy et al. Experimental results show that the fusion zone features cellular and cellular-dendrite crystal structure, HAZ mainly exhibits equiaxed crystals, and near the fusion zone the equiaxed crystals coarsen. With the increase of power input and pulse duration for laser, the penetration ratio and melted metal width increase, and microstructures of the weld metal and HAZ have coarsening tendency. It is unfavorable to select short pulse duration (2 ms, 3 ms) for controlling welding quality. The highest tensile strength of laser-welded joints reaches to 680 MPa (pulse duration of 10 ms and power input of 7.6 J), the weld centre being the weakest region in the joints.

Key words: austenite stainless steel wire; laser welding; joint microstructure; mechanical properties

Wettability of Sn-9Zn-*x*Ag lead-free solder and mechanical properties of soldered joints

CHEN Wenxue, XUE Songbai,

WANG Hui, WANG Jianxin (College of Materials Science and Technology, Nanjing University of Aeronautics and Astronautics, Nanjing 210016, China). p 75—78

Abstract: The effects of Ag on the wettability of Sn-9Zn lead-free solder and the mechanical properties of soldered joints are investigated respectively. The results indicate that when the content of Ag is 0.3 wt.%, the solder gets the best wettability; when the content of Ag is from 0.5 wt.% to 1 wt.%, the wettability decreases. The best mechanical property of soldered joint is obtained when the content of Ag is 0.3 wt.%. Moreover, the fracture micrographs show that plenty of dimples are found on the Sn-9Zn-0.3Ag soldered joints fractures. When the content of Ag is 1 wt.%, some Cu-Zn and Ag-Zn intermetallic compounds appear on the bottom of dimples, and the mechanical property of the soldered joint decreases. In general, the optimum additive amount of Ag in Sn-9Zn solder is about 0.3 wt.%.

Key words: Ag; lead-free solder; wettability; mechanical property

Genetic algorithm of grain growth in heat-affected zone of 45 steel AC flash butt welding ZHANG Genyuan, XU Maili, TIAN Songya, Wen Fang (College of Mechanical & Electrical Engineering, Hohai University, Changzhou 213022, China). p 79—82, 86

Abstract: The austenite grain growth process of 45 steel in AC flash butt welding heat-affected zone (HAZ) was simulated by genetic algorithm method based on actual measured welding thermal cycle curves, which the energy of the system in minimum state and the grain boundary moved to curvature direction in grain growth process were considered. The average radius actually measured in coarse grain area and fine grain area of welding HAZ are 54.30 μm and 13.58 μm, and agree with the average grain radius of 51.50 μm and 16.29 μm simulated by genetic algorithm simulation method. Genetic algorithm method results show the average radius of grain growth in welding HAZ during welding heat recycles is 66.8 percent of that during the whole heat.

Key words: genetic algorithm; grain growth; welding heat-affected zone; simulation

Effect of post-weld heat treatment on microstructure and mechanical property of manual SHS welding XIN Wentong[1,2], MA Shining[1], LI Zhizun[2], ZHANG Baoyuan[2] (1. National Key Laboratory for Remanufacturing, Armored Force Engineering Academy, Beijing 100072, China; 2. Base Department, Ordnance Engineering College, Shijiazhuang 050003, China). p 83—86

Abstract: The influences of post-weld heat treatment on microstructure and mechanical properties of manual SHS welding at different temperatures are studied. The results indicate that the diffusion activation ability of elements can be reached when the annealing temperature is more than 300℃. With the increasing of temperature, the tensile strength and the impact toughness of the welded joint improve, the micro-hardness gaps near the fusion line of the base metal and the welded alloy reduce, and the microstructures in the fusion area distribute uniformly. Through spread scanning of the element by the EDS energy spectrum, the concentration change of the major elements in the fusion area is found out, which is from mutation form before the post-weld heat treatment into gradient form and strengthens the intensity of the fusion zone.

Key words: manual SHS welding; microstructure; mechanical property; post-weld heat treatment

TIG arc behavior of ultrafast-convert high-frequency variable-polarity square wave CONG Baoqiang, QI Bojin, ZHOU Xingguo (School of Mechanical Engineering and Automation, Beijing University of Aeronautics and Astronautics, Beijing 100191, China). p 87—90

Abstract: Based on a novel main circuit topology of ultrafast-convert power supply, variable polarity current with the ultrafast current rate of rise and fall was achieved, and the arc behavior of high-frequency variable-polarity tungsten inert-gas welding for aluminum alloy was investigated. The experimental results show that with the increase of current frequency, the cleaning action of ultrafast-convert high-frequency variable-polarity arc for surface oxide is significantly enhanced, arc plasma has an obvious pinch effect, arc voltage and arc resistance increase respectively, but arc blow-effect is also enhanced. Increasing the current frequency and decreasing negative polarity current amplitude and its duration in certain ranges can improve weld penetration and reduce the electrode consumption. It is beneficial to improve weld quality and efficiency for aluminum alloys.

Key words: ultrafast convert; ultrasonic; variable polarity; arc behavior; pinch effect

Properties of 45 carbon steel hardened by micro-plasma WANG Liuying[1,2], LIU Gu[1], HUANG Guoperg[3], HUA Shaochun[1] (1. The Second Artillery Engineering College, Xi'an 710025, China; 2. Key Laboratory of Electronic Ceramics and Devices of Ministry of Education, Xi'an Jiaotong University, Xi'an 710049, China; 3. The Second Artillery Commissary, 7435 Factory, Wuhan 432100, China). p 91—94

Abstract: Uniform experiment design was applied to hardened 45 carbon steel with micro-plasma arc, including the design parameters such as arc current, scanning speed, gas flow and hardening distance. The structures, mechanical properties and hardening mechanism of hardened layers were analyzed by means of testing instruments such as optical microscope, scanning electron microscope, microhardness tester and wear tester. Results show that because of the small influencing area and the extremely high cooling